2010 IEEE International Conference on Robotics and Automation
Anchorage Convention District
May 3-8, 2010, Anchorage, Alaska, USA

Precise robot motions using dual motor control

Sven Gestegård Robertz*, Lorenz Halt*, Sameer Kelkar***, Klas Nilsson*
Anders Robertsson**, Dominique Schär***, Johannes Schiffer**

Abstract— **High motion performance, stiffness, and accuracy are crucial for industrial robot applications, but these requirements are in practice contradictory. Using a novel type of robot, the so called Gantry Tau, new combinations of stiffness and accuracy are in principle possible, except for the backlash in the drive-trains of each joint.**

Existing techniques for backlash reduction are either mechanically complex or limit the mechanical bandwidth. This paper presents an approach based on dual motors connected in parallel to the load, such that the entire robot structure can be made practically backlash free by means of software and feedback control.

Different control strategies are presented and evaluated in experiments ranging from a lab servo process via a table-sized robot to a large industrial implementation with several meters of working range. Special emphasis was on a dual motor test rig with a linear high-resolution scale (not yet used for feedback) where the combined motor torque was fully utilized for high acceleration, while reducing backlash by over 96%.

I. INTRODUCTION

In order to complement human workers, we want robots that are fast (high acceleration), accurate (repeatability), stiff (with respect to process forces), and have a large working range. For productivity there are also the needs for low cost, and low end-effector inertia in combination with the desired stiffness, which results in a high mechanical bandwidth as needed for high-performance force-controlled interaction with the environment. For many applications parallel kinematic manipulators (PKMs) represent an approach to accomplish many of these needs, but traditionally such robots have had a small/closed workspace [15]. In that perspective the so called Tau PKM principle is a breakthrough in that it combines the other advantages with a large/open workspace [12], [5], [4]. The remaining issue, which is the topic of this paper, then is the (absolute/calibrated as well as repetitive) accuracy.

Within the EU FP-6 project SMErobot™ the needs for low cost and high stiffness with respect to process forces excluded direct drive robots. Instead, the use of the Gantry Tau principle (depicted in Fig. 1 and Fig. 2) with linear motions built on *rack-and-pinion linear motions with motors driving via planetary gearboxes* was identified as the optimum design. With backlash-free ball-joints, the only remaining backlash is in the drive-train, and hence that is the issue to resolve. In the following we focus on accuracy for PKMs, but the same principles should (with lower stiffness or higher inertia) apply for articulated arms as well.

Fig. 1. The full-scale F1 Parallel Kinematic Manipulator at Güdel AG, Langenthal, with dual motor control on each cart for overall increased accuracy and stiffness.

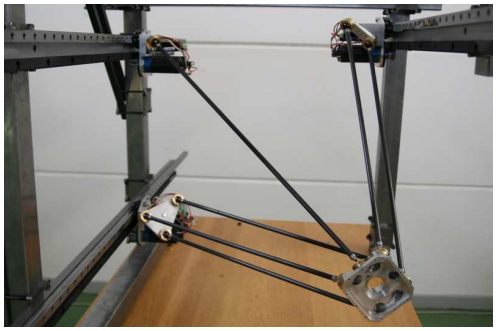

Fig. 2. The T1 Parallel Kinematic Manipulator at the robot lab in Lund.

The approach is to reduce these effects by using two motors for each cart of the linear motion, instead of the conventional use of only one motor per degree of freedom. This paper compares the different control strategies considered, and presents experimental evaluation on both small-scale test rigs and a full-size industrial robot. A model of non-linearities including backlash, and the effects of the additional motor on system performance and stability analysis is reported in [20].

* Department of Computer Science, Lund University, Sweden.
Contact: {sven,klas}@cs.lth.se.
** Department of Automatic control, Lund University, Sweden.
Contact: andersro@control.lth.se.
***Güdel AG, Langenthal, Switzerland.
Contact: Dominique.Schaer@ch.gudel.com.

This work was partially performed within the EU FP6 project SMErobot™ under grant no. 011838, and the SSF project ENGROSS.

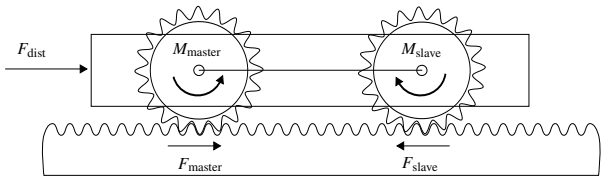

Fig. 3. Principle of using two cooperating motors to minimize backlash.

II. DUAL MOTOR CONTROL

Backlash and dead-zones are phenomena which are present in all mechanical robot systems and which may severely deteriorate the performance of tracking and positioning accuracy, in particular in the presence of unknown load disturbances and friction, where also stability problems such as undesired limit-cycles may occur.

Several descriptions of backlash and control of systems with backlash have been reported in the literature, see e.g., [19], [2], [17], [18], [14] and references therein.

Some previous work and preliminary results on dual motor control for a parallel robot was reported in [3]. Related approaches for backlash reduction have been published in the areas of antennas [8], tracking platforms [10] and servo-systems [6].

Rather recently a new dynamic model of backlash capturing the main properties was derived by Nordin and Gutman, see [17], [16]. That model has been used in the analysis and design of the presented controllers.

Fig. 3 shows the principle of using two cooperating motors, mounted in parallel to the same load, to reduce backlash. We will now present three possible implementations of that principle; using the second (*slave*) motor as (A) a spring providing constant torque, (B) using a position offset to generate a corresponding torque when close to the position setpoint, and (C) a more holistic non-linear control strategy.

A. Constant torque reference

To reduce the backlash effect and achieve a stiff behavior against disturbances, one motor should act like a rotational spring to close the gap. To prove the concept and to study the behavior of the control, the second drive is set to torque control with a constant setpoint. The value of the constant torque is significant for the results. It must be high enough to overcome friction and be able to close the backlash gap, but cannot be too high or it will severely restrict the performance of the position control.

The slave drive is set to a constant torque, $M_{\text{slave}} = const$. After reaching one side of the backlash, the force F_{slave} pushes the pinion of the master drive. When both pinions are in contact with the rack, the integral part of the master controller will cancel out the constant force F_{slave}. In steady state $M_{\text{master}} = M_{\text{slave}}$. Considering disturbance forces $|F_{\text{dist}}| > |F_{\text{slave}}|$, the behavior of the cart position has to be distinguished depending on the sign of F_{dist}. If $\text{sign}\,(F_{\text{dist}}) = -\text{sign}\,(F_{\text{slave}})$, the master drive will be able to control the torque M_{master} to react on the disturbance. If $\text{sign}\,(F_{\text{dist}}) = \text{sign}\,(F_{\text{slave}})$, the constant torque may be overcome and the pinion of the master drive will lose contact with the rack. The system will be uncontrollable until the opposite side of the gap is reached. When there no longer is a disturbance the cart will return to the desired position again.

B. Position reference offset

A big drawback of the constant torque strategy is that the slave motor does not contribute to moving the cart, which wastes energy. A more efficient controller should use both motors for maximum acceleration when being far from the position setpoint, and the 'slave motor' should only provide the antagonistic torque when close to the target.

That can be achieved by disabling any integral action in the slave controller and adding a small offset to the position setpoint fed to the slave. Without integral action, the controller output is constant for a constant difference between the setpoint and final position; the antagonistic torque used to eliminate backlash. Thus, if an appropriate offset in the rotational position of the slave drive is chosen, the master position control cascade (with integral action) will drive the cart to a stationary accurate final position while the offset in the slave drive will result in the torque M_{slave}.

This strategy is easy to implement using standard servo drives, as the only coupling between the two controllers is the mechanical connection. The position offset, however, depends on the initial position in the backlash and must be found for every start-up. The offset can be determined as follows: Both drives start at initial positions. The master position setpoint is kept constant while the slave setpoint is increased until the torque reference reaches the desired value.

The chosen final torque reference determines the capability to close the backlash gap and therefore the accuracy of the control. Because of the indirect regulation any uncertainty in position estimation will affect not only the system response during movement but also the stiffness in end position. Furthermore two dynamical systems work against each other in steady state. Care must be taken when assigning parameter values in order to avoid transient variations in the cart position.

Considering Fig. 3, the force $F_{\text{slave}}$is now determined through a constant error in its position setpoint. If $\text{sign}\,(F_{\text{dist}}) = -\text{sign}\,(F_{\text{slave}})$ both drives will work against the disturbance force. If the cart is moved due to the disturbance, F_{slave} gets stronger since the error to the setpoint of the slave drive will get bigger. If $\text{sign}\,(F_{\text{dist}}) = \text{sign}\,(F_{\text{slave}})$, F_{dist} and F_{slave} will sum up. In this case, if the cart is actually moved due to the disturbance force, F_{slave} will decrease.

C. A non-linear controller

A more advanced technique is the so called *Switching Strategy* [20]. The principle is that both drives run position control individually when far from the target position. When approaching the final position the slave controller will be seamlessly faded from position control to pure torque control with a constant setpoint. In this way, the backlash gap is

closed and high accuracy in the final cart position can be achieved. The switching parameter $\mathrm{v_{sw}}$ is used to enable a smooth transition between position and torque control for the slave drive.

III. THE SWITCHING CONTROLLER

The switching controller is an attempt to address the trade-off between efficiency and accuracy. For efficiency, all available motor power should be utilised for high motion performance, but for accuracy the motors must work in opposite directions when close to the final position, to close the backlash gap. The switching controller is a non-linear control strategy with such behaviour, implemented as two coupled cascaded controllers.

The principle of operation is to divide a step response into three different behavioural phases. During the first phase a fast movement is intended and both drives are running pure position control, working in the same direction. The second phase is a smooth transition from position control to torque control of the slave drive. During this phase the position controller output is faded out and replaced by a constant torque setpoint in the reverse direction. In the third and final phase, the slave drive will only be torque controlled and work against the position controlled master drive, behaving similar to a rotational spring and ensuring physical contact to either one side of the backlash gap.

A. Switching Strategy

The transient second phase is the most critical one, because a continuous switch from position- to torque control of the slave drive is desired. By introducing a function $\mathrm{v_{sw}}$ that determines the percentage of the replacement, a continuous switching, easy to parametrize, can be achieved. We will now present a switching strategy acting on the relative setpoint error e_{abs},

$$e_{\mathrm{abs}} = \frac{|x_{\mathrm{ref,new}} - x_{\mathrm{meas}}|}{|x_{\mathrm{ref,old}} - x_{\mathrm{ref,new}}|}. \tag{1}$$

This option utilises the knowledge that the main influence of the backlash angle occurs when the cart is reaching its final position. This is manifested by the arise of possible limit cycles. The switching function is defined as

$$\mathrm{v_{sw}} = \begin{cases} 0, & e_{\max} < e_{\mathrm{abs}} \\ \mathrm{sign}\left(\Delta x_{\mathrm{ref}}\right) \frac{e_{\mathrm{abs}} - e_{\max}}{e_{\min} - e_{\max}}, & e_{\min} \le e_{\mathrm{abs}} \le e_{\max} \\ \mathrm{sign}\left(\Delta x_{\mathrm{ref}}\right), & e_{\mathrm{abs}} < e_{\min}, \end{cases} \tag{2}$$

with $\Delta x_{\mathrm{ref}} = x_{\mathrm{ref,old}} - x_{\mathrm{ref,new}}$ and $e_{\min}$ and $e_{\max}$ as user parameters. The function $|\mathrm{v_{sw}}| = |f(e_{\mathrm{abs}})|$ is shown in Fig. 4.

By adding two functional blocks as illustrated in Fig. 5 the switching module can be included into the slave drive control cascade. One block multiplies the constant torque reference value M_{const} with the sign of the switching variable $\mathrm{v_{sw}}$. The other block multiplies the input with the absolute value $\mathrm{v_{sw}}$. One can see in Fig. 5 that if $|\mathrm{v_{sw}}| = 0$ there will be no influence by the switching module but if $|\mathrm{v_{sw}}| = 1$ the setpoint coming from the velocity control will be totally replaced by the constant value $M_{\mathrm{const}} \cdot \mathrm{sign}\left(\mathrm{v_{sw}}\right)$.
Since the relative error e_{abs} is dependent on the cart position, the calculation of $\mathrm{v_{sw}}$ according to Equation (2) is done by the *global handler* instance as described below.

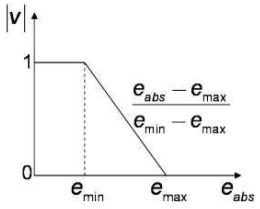

Fig. 4. Switching function $\mathrm{v_{sw}} = f(e_{\mathrm{abs}})$. The parameters $e_{\min}$ and $e_{\max}$ are the fractions of the step between which the slave controller is faded from position to torque control; as e_{abs} decreases, the slave controller changes from position to torque control.

B. Control Structure

The control is implemented with cascaded torque, angular velocity, and position controllers, which offers a good structure for both feedback control and model-based feedforward. Integral action in one of the controllers is needed to ensure stationary convergence, and it is industrial standard for servo controls to include the integral part in the velocity control loop. That enables the cascade to cancel out stationary errors in both the position and velocity control loops. Errors after the *I*-part are manageable with feedforward techniques. Furthermore, for robotics applications, there must be no overshoot in the position control, which is achieved by having a purely proportional position controller. For the torque loop, proportional control allows both fast reaction and fast calculations.

The I-part in the velocity loop will dampen the control and make it more robust to noise, which is expected due to position derivation. The overall structure is illustrated in Fig. 5. A global reference value for the cart position is set by the user and then scaled with the gear-ratios r_{pinion} to get rotational position for each drive, according to

$$\varphi_{\mathrm{ref},1..2} = \frac{1}{r_{\mathrm{pinion}}} x_{\mathrm{cart,ref}} + \bar{\varphi}_{1..2}. \tag{3}$$

with offsets $\bar{\varphi}_{1..2}$ set by calibration or for homing functionality.

In fact, the *global handler* instance could be used as an additional controller using measurements from a high-resolution linear scale along the rails in future applications. In our experimental setup that sensor was only used for evaluation. As discussed in [1], control structures that include more than one integral action in parallel, will lead to loss of observability and controllability, and may cause drift and unstable subsystems. In case of any disturbances it is thus not possible to change both output signals individually with respect to the error. Since the uncontrollable state is an integrator it will not decrease to zero but stay at an arbitrary value. The authors propose to use one integral state and

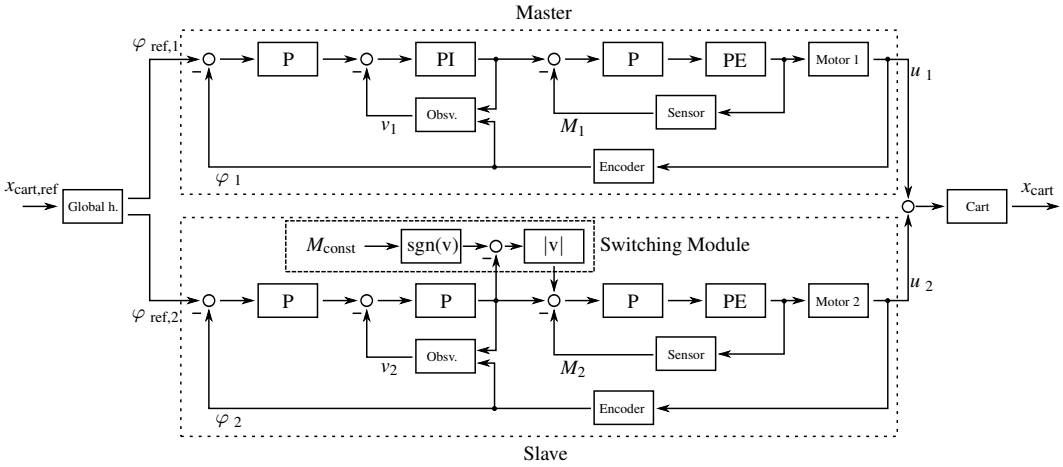

Fig. 5. Block diagram of the dual motor controller.

distribute its output to all drives if necessary. Consequently in the sequel only the upper cascade includes integral action within the velocity controller. It is named *master drive*, while the lower cascade without integral action but including the *switching module*, is labeled *slave drive*. The two cascades differ in structure only with respect to the I-part within the velocity controller, but will typically contain different control parameters. Obviously, the slave drive additionally includes the switching module described above. However, with some mechanical compliance (i.e., added dynamics) between the two drives, it is still possible to use integral parts in both controllers and a careful offset in references, as done in the presented F1 experiments.

C. Stability analysis - a short sketch

This section contains a short outline for the stability analysis of the suggested controller structure. A full proof with conditions and numerical values for stabilizing controller parameters is available in [20].

The controlled servo system in Fig. 5 can be written as a feedback-connection of a linear system $G(s)$ (including servo and controller dynamics) and the nonlinear backlash elements as shown in Fig. 6. The static part of the backlash for each drive can modeled by a dead-zone, $dz(\cdot)$;

$$dz_{2\alpha}(\Theta_d) = \begin{cases} \Theta_d - \alpha, & \Theta_d > \alpha, \\ 0, & |\Theta_d| < \alpha, \\ \Theta_d + \alpha, & \Theta_d < -\alpha \end{cases} \tag{4}$$

The input u_3 in Fig. 6 corresponds to the braking torque M_{const} of the slave drive, and is used to close the backlash gap. For $u_3 = 0$ it is straightforward to show that there will be non-unique equilibria within the deadzones, whereas for $u_3 \neq 0$ one can obtain an equilibrium point outside the deadzones. Local stability of the equilibrium for $u_3 = M_{const} \neq 0$ can be analysed via a shift of equilibrium to the origin followed by eigenvalue analysis of the corresponding system matrix.

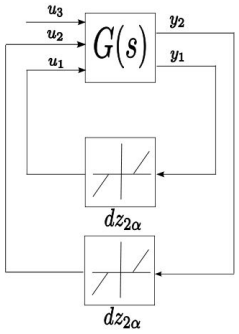

Fig. 6. Feedback connection of a linear subsystem and backlash/dead-zone nonlinearities where u_3 corresponds to the braking torque M_{const} in Fig. 5.

For global stability analysis of the closed loop system, we use the multivariable circle criterion, *cf.* [13], which can be applied to the feedback connection of a linear subsystem and cone bounded nonlinearities. The braking torque will shift the equilibrium and thereby also change the sector bound(s) for the nonlinear elements. By performing a loop transformation the system is put into a standard form for analysis and sufficient conditions on the magnitude of M_{const} are derived which guarantee global stability of the equilibrium. It should be noted that these bounds may be conservative, and that both simulations and experiment show good results also for a larger range of brake torques.

IV. EXPERIMENTAL RESULTS

The presented dual-motor control was experimentally evaluated in terms of accuracy and stiffness.

A. Lab experiment: servo with backlash

The first experiment studies the performance of the switching strategy without load disturbances. The process, shown in Fig. 7, consists of two equal rotating masses, the backlash element and two equal DC motors of which one is used

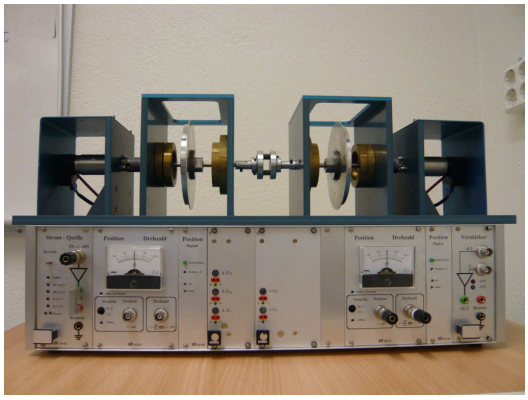

Fig. 7. Experimental setup with the mass representing the motor on the right and the load on the left side. The backlash element is situated in the middle.

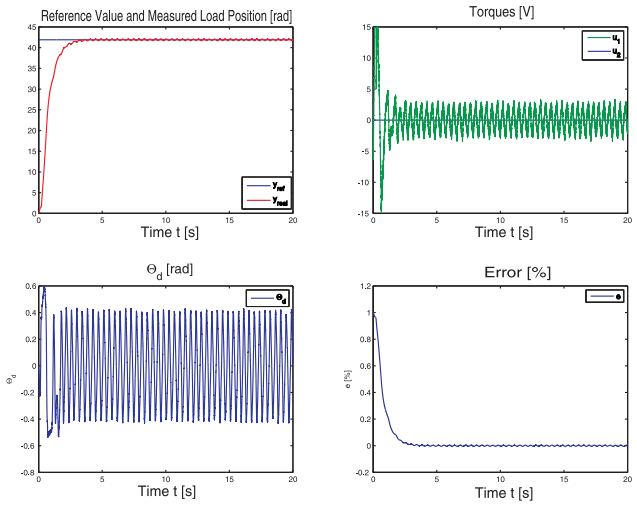

Fig. 8. Experimental step response with single motor ($u_2 = 0$). The backlash causes limit cycles.

as the driving (master) motor and the other one (slave) is used on the load side. The shaft does not include a spring element, and the backlash is approximately 30 degrees. This is an exaggerated lab process used to isolate the backlash phenomena for experimental purposes.

Fig. 8 shows how the backlash causes limit cycles when running single motor control. Fig. 9 shows the input, outputs, and the switch variable of the backlash servo during a step response. The system shows no limit cycles and no negative response behavior.

B. Lab experiment: T1 gantry robot linear axis

A tabletop experimental setup with Faulhaber DC micromotors and a THK linear guide was used to evaluate and compare different control strategies. A constant position reference is set, the cart is subjected to external disturbances, and the resulting position after the disturbance is removed is studied. The actual cart position is measured using a Heidenhain LIDA 487 linear scale with $0.4\,\mu m$ resolution attached along the beam of the linear motion, as illustrated

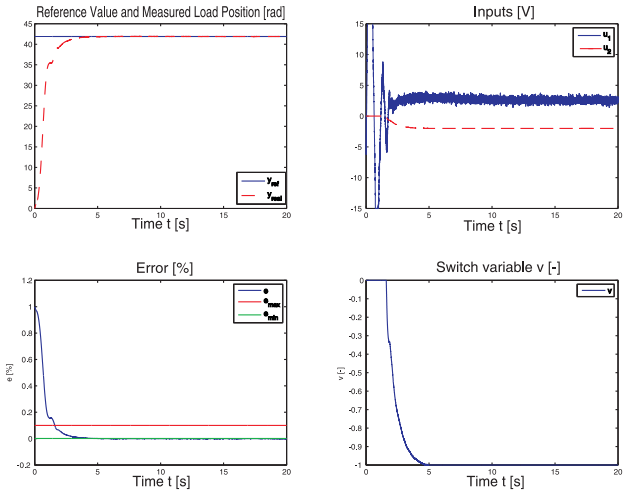

Fig. 9. Experimental step response with the switching controller ($M_{slave} = f(e_{abs})$). u_1 is the input to the master motor and u_2 to the slave.

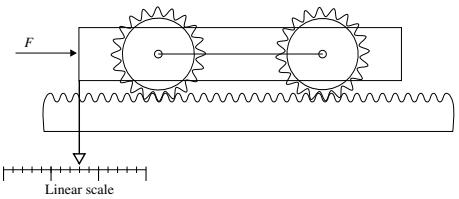

Fig. 10. The position of the cart is measured using an external linear scale, and the disturbance force is measured by a force/torque sensor attached to the cart.

in Fig. 10. A photo of the setup is shown in Fig. 11. An ATI mini85 force sensor at one end of the cart measures external disturbances. The linear position of the cart and the disturbance force is monitored and evaluated using a real-time MATLAB/Simulink model [11].

1) Baseline: Single motor control: To provide a base line for comparison, the stiffness and backlash of the system with just a single motor attached to the rack was measured, and the results can be seen in Fig. 12 and Fig. 13. The maximum difference in position is $\Delta p_{\max} = 607.2\,\mu\mathrm{m}$, and the stiffness of the system when the gears are engaged is approximated to $\tau = 15.6\,\mathrm{N}/\mu\mathrm{m}$.

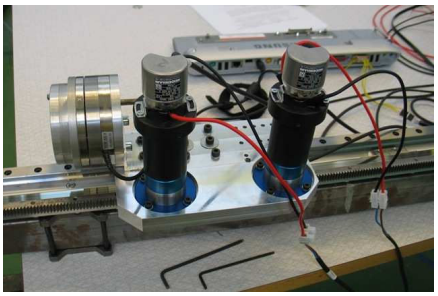

Fig. 11. The testbed consisting of a cart with dual motors on a linear axis, a high-resolution linear measurement scale along the rail, and a force/torque sensor for force measurements.

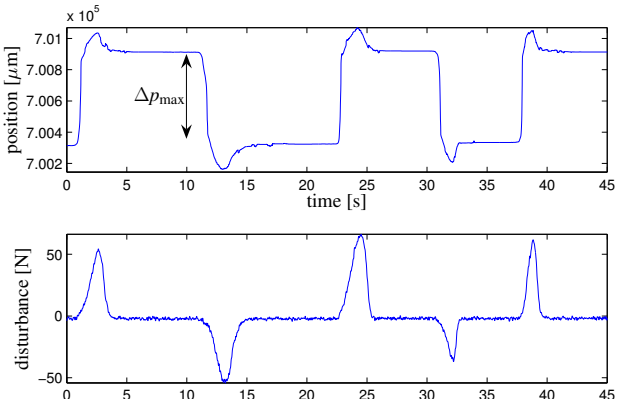

Fig. 12. Experimental measurements on the single motor control with external disturbances. The cart can move within the backlash gap when the pinion loses contact with the rack.

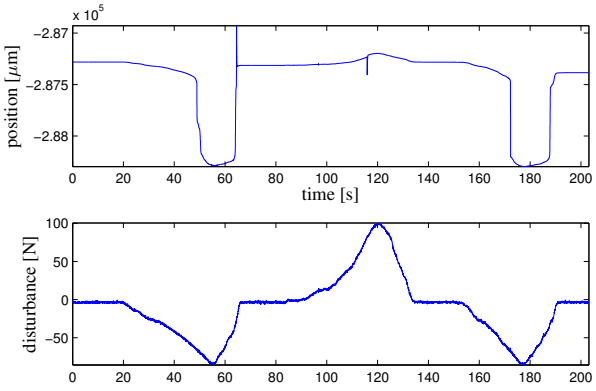

Fig. 14. Experimental measurements on the constant torque system. The pinion stays in contact with the rack.

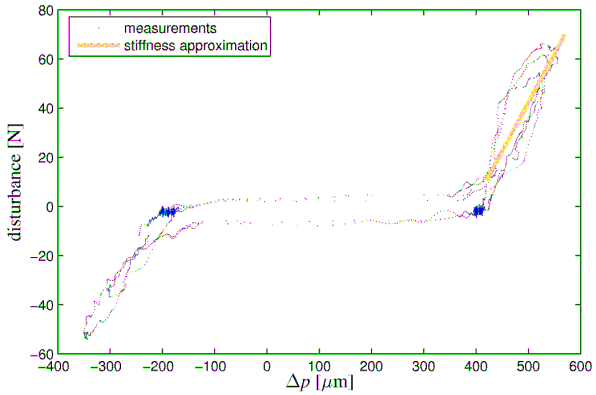

Fig. 13. Stiffness measurements for the single motor system. The backlash causes hysteresis as the system is not controllable within the gap.

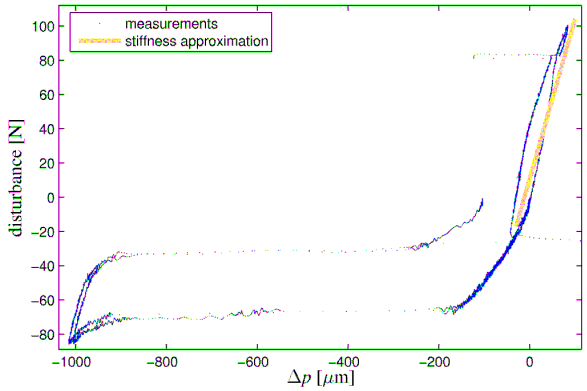

Fig. 15. Stiffness measurements for the constant torque controller

2) Constant torque reference: The result when using one of the motors to provide constant torque is shown in Fig. 14 and Fig. 15. The torque reference was $3.0\,\mathrm{Nm}$ ($F_{slave} \approx 160\,\mathrm{N}$, and hysteresis between $\Delta p_{\max} = 40\,\mu\mathrm{m}$ and $\Delta p_{\max} = 88\,\mu\mathrm{m}$ was observed. The stiffness was approximated to $\tau = 26.9\,\mathrm{N}/\mu\mathrm{m}$.

3) Position reference offset: The result for the dual motor control with position offset is shown in Fig. 16 and Fig. 17. Backlash is reduced to $\Delta p = 63.6\,\mu\mathrm{m}$ and stiffness in one direction is approximated to $\tau = 31\,\mathrm{N}/\mu\mathrm{m}$.

4) Switching controller: Results from reference changes using the non-linear switching dual motor controller described in Sec.III are shown in Fig. 18 and Fig. 19. The backlash is reduced to $\Delta p_{\max} = 32.4\,\mu\mathrm{m}$ and the stiffness in both directions is approximated to $\tau = 29\,\mathrm{N}/\mu\mathrm{m}$.

5) Repeatability (switching controller): In addition to the load disturbance experiments, repeatability was measured performing small step responses, as shown in Fig. 20. The measured bidirectional repeatability was $\Delta p_{\max} = 51.6\,\mu\mathrm{m}$, and unidirectional repeatability was $\Delta p_{\max} = 4.5\,\mu\mathrm{m}$.

C. F1 full-scale prototype

For comparison, and to indicate how the presented approach scales to larger machines, we will now summarize measurements of the stiffness and repeatability of the F1 robot, see Fig. 1, performed at Güdel AG, Langenthal [7]. The dual motor control currently used for the F1 PKM prototype is done using the position offset strategy.

As shown in Fig. 21 the average error in uni-directional repeatability was found to be $0.003\,\mathrm{mm}$ and the maximum error observed was $0.007\,\mathrm{mm}$ (through 97 points). This was is the same range as the accuracy of the laser tracker being used to measure the machine. Therefore, limited gauge testing (2 positions only) was performed utilizing a dial gauge of a single micron resolution. During this limited testing, the uni-directional repeatability of the machine was found to be of the order of 1 micron.

The F1 stiffness in-line with the linear axes varies from $1.15\,\mathrm{N}/\mu\mathrm{m}$ (on corners) to $2.5\,\mathrm{N}/\mu\mathrm{m}$ (center point). For external load forces at the *tool center point* (TCP) in the direction towards the rail of the "triple link", see Fig. 1, the stiffness varies from $0.68\,\mathrm{N}/\mu\mathrm{m}$ to $1.8\,\mathrm{N}/\mu\mathrm{m}$. With load forces in the direction towards the rail of the "double link", the stiffness is approximately uniform at $0.6\,\mathrm{N}/\mu\mathrm{m}$ around the workspace. This lower stiffness can be explained because it is in the direction of the leg with the single link only due to the 3/2/1 configuration of the manipulator.

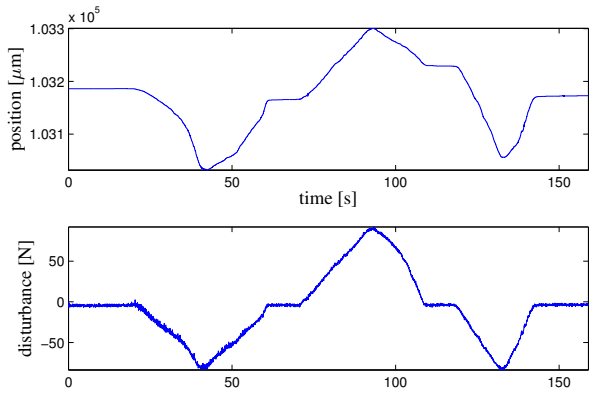

Fig. 16. Experimental measurements on the position offset controller. The backlash was reduced to $\Delta p_{\max} = 63.6\,\mu$m.

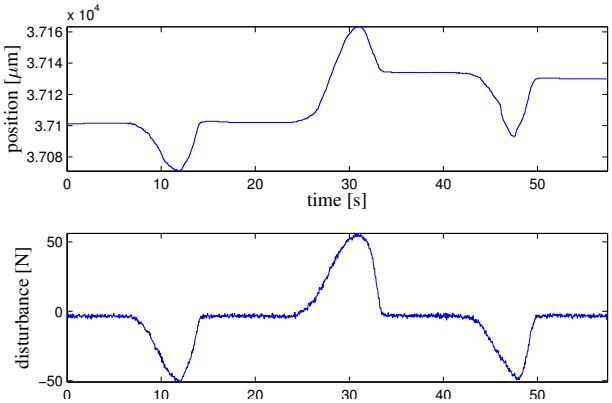

Fig. 18. Experimental measurements on the switching controller. The backlash was reduced to $\Delta p_{\max} = 32.4\,\mu$m.

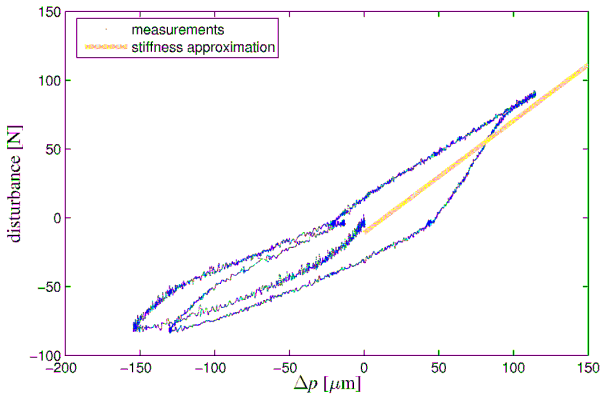

Fig. 17. Stiffness measurements for the position offset controller

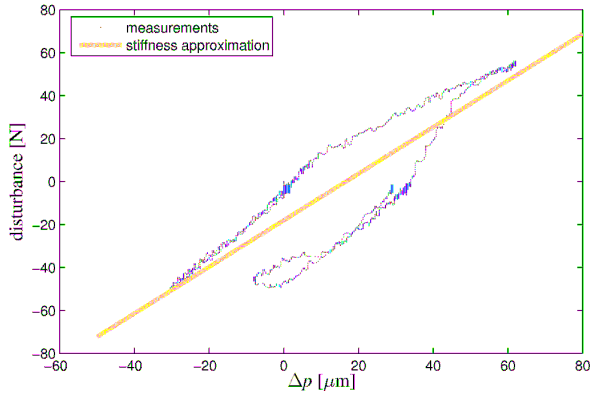

Fig. 19. Stiffness measurements for the switching controller

V. DISCUSSION

The presented approach to backlash elimination by dual-motor control is a first proof-of-concept, and while the results are very promising and the technique yields a big improvement over single motor control, we make no claims of optimality. The switch functions considered — from co-acting motors in an acceleration phase to counteracting to cancel backlash — is one of many possible approaches.

In particular, the presented controllers do not include any internal model of external forces. Our future work includes finding an optimal control strategy taking process forces into account.

In the experiments with the T1 linear axis, there is a positioning inaccuracy (Δp), which is significantly larger than the resolution of the rotary encoders. The master drive (which has the integral action) does, however, not see this error — it reaches its target position to the encoder increment. As seen from the experiments, the unidirectional repeatability is significantly better than the bidirectional.

That effect appears to be caused by mechanical compliance that becomes apparent as the direction of the slave torque depends on the direction of the reference step. One method of mitigating this is to identify or model the mechanics, to be able to compensate for the known deflection for a given torque. A more straight forward enhancement would be to include feedback from the external linear scale, here used for evaluation only, in order to improve both accuracy and stiffness. However, adding an external linear scale of course increases the cost of a machine.

In the presented experiments on the F1 full-scale prototype, the position offset strategy was used instead of the switching controller. The reason for this is that the position offset controller performs almost as well, and is much easier to implement using off-the-shelf servo drives, as it requires no communication between controllers. The F1 experiments were primarily aimed at studying the mechanical stiffness, and thus the added effort of implementing the switching controller could not be justified.

From an application perspective, absolute accuracy is paramount. The high mechanical bandwidth of the robot makes it much more suitable for stiff contact force control tasks than ordinary serial manipulators, e.g, in grinding and fettling applications in foundry industry. Further features are low actuator power and energy consumption, due to the low inertia and the non-redundancy of the robot, which makes it easy to assemble and disassemble without the need of complicated mechanical adjustment procedures. However, there needs to be efficient calibration methods to guarantee the absolute accuracy of the manipulator. The kinematics,

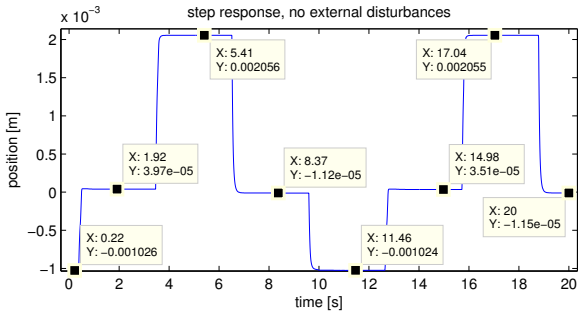

Fig. 20. Step response without external disturbances, using the switching controller. The position is measured using the external linear scale which is not used for control. Bidirectional repeatability is $\Delta p_{\max} = 51.6\,\mu\text{m}$, and unidirectional repeatability is $\Delta p_{\max} = 4.5\,\mu\text{m}$.

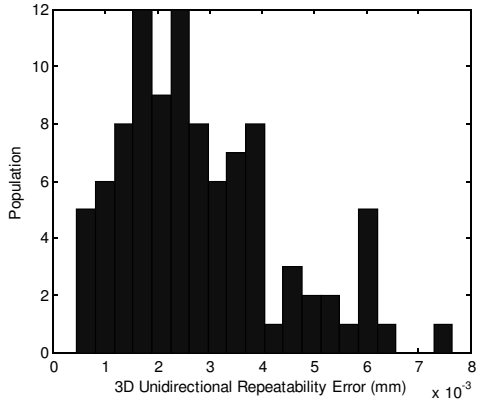

Fig. 21. Unidirectional repeatability of the TCP of the F1 PKM with 5 axis motion.

calibration and application areas are described in [9], [7]. Clearly, powerful calibration is more meaningful when backlash effects are eliminated.

VI. CONCLUSION

Different approaches to reduce backlash effects using dual motor control strategies have been presented and experimentally verified. A constant force in-between two cooperating motors ensures contact of drives and load. The presented dual motor control strategies utilize the redundancy of two motors to achieve both high speed movement and stiff and precise position control.

Dramatic backlash reduction of $85.5\,\%$ of the maximum backlash gap could be achieved by applying constant torque. The presented dual motor control strategies gave further improvement, reducing backlash with $89.5\,\%$ with the *Position Offset Strategy* and $96.9\,\%$ with the *Switching Strategy*. The position uncertainty for each strategy is illustrated in Fig. 22. These results prove the potential of dual motor control strategies for high-speed and high-precision robotic applications.

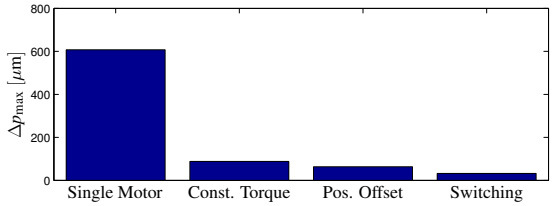

Fig. 22. Backlash for the different controllers

REFERENCES

[1] Karl Johan Åström and Tore Hägglund. *Advanced PID Control*. ISA - The Instrumentation, Systems, and Automation Society, Research Triangle Park, NC 27709, 2005.

[2] G. Brandenburg and U. Schäfer. Influence and adaptive compensation of simultaneously acting backlash and Coulomb friction in elastic two-mass systems of robots and machine tools. In *Proc. ICCON'89*, pages WA–4–5, Jerusalem, 1989.

[3] Benoit Brochier. Control of a Gantry-Tau structure. Master's Thesis ISRN LUTFD2/TFRT--5777--SE, Department of Automatic Control, Lund University, Sweden, July 2006.

[4] T. Brogårdh. A device for relative movement of two elements, 1996. Patent WO 97/33726.

[5] T. Brogårdh, S. Hanssen, and G. Hovland. Application-oriented development of parallel kinematic manipulators with large workspace. In *Proc. of the 2nd International Colloquium of the Collaborative Research Center 562: Robotic Systems for Handling and Assembly*, pages 153–170, Braunschweig, Germany, 2005.

[6] G.H. Choi, H. Nakamura, and H. Kobayashi. Calibration of servo systems with redundant actuators. In *Proceedings of IFAC world congress*, pages 169–174, San Francisco, CA, 1996.

[7] P.J. Crothers, P.L. Freeman, I. Dressler, K. Nilsson, A. Robertsson, W. Zulauf, B. Felber, R. Loser, K. Siercks, and T. Brogårdh. Characterization of the tau parallel kinematic machine for aerospace application. *SAE International*, 2009. 09ATC-0203.

[8] W. Gawronski, J.J. Beech-Brandf, Jr. H.G. Ahlstrom, and E. Maneri. Torque-bias profile for improved tracking of the deep space network antennas. *IEEE Antennas and Propagation Magazine*, 42(6), 2000.

[9] Mathias Haage, Isolde Dressler, Anders Robertsson, Klas Nilsson, Torgny Brogårdh, and Rolf Johansson. Reconfigurable parallel kinematic manipulator for flexible manufacturing. In *Proc. 13th IFAC Symposium on Information Control Problems in Manufacturing (INCOM2009)*, June 3 - 5, 2009, Moscow, Russia, June 2009.

[10] Z. Haider, F. Habib, M.H. Mukhtar, and K. Munawar. Design, control and implementation of 2-dof motion tracking platform using drive-anti-drive mechanism for compensation of backlash. In *IEEE International Workshop on Robotic and Sensors Environments*, 2007.

[11] Lorenz Halt. Implementation and evaluation of accurate and stiff position control for a parallel kinematic robot. Master's thesis, Dept. of Computer Science, Lund University (LTH), Sweden, 2009.

[12] L. Johannesson, V. Berbyuk, and T. Brogårdh. Gantry-Tau – a new three degrees of freedom parallel kinematic robot. In *Parallel Kinematic Machines in Research and Practice; The 4th Chemnitz Parallel Kinematics Seminar*, pages 731–734, 2004.

[13] H.K. Khalil. *Nonlinear systems*. Prentice Hall, N.J, 3rd edition, 2002.

[14] A. Lagerberg. A literature survey on control of automotive powertrains with backlash. Technical report, Control and Automation Laboratory, Department of Signals and Systems, Chalmers University of Technology, Göteborg, Sweden, 2001.

[15] J.-P. Merlet. *Parallel Robots*. Kluwer Academic Publishers, MA, 2000.

[16] M. Nordin. *Nonlinear backlash compensation for speed controlled elastic systems*. PhD thesis, Division Optimization and Systems Theory, Department of Mathematics, The Royal Institute of Technology, Stockholm, Sweden, 2002.

[17] M. Nordin and P.-O. Gutman. Controlling mechanical systems with backlash - a survey. *Automatica*, 38:1633–1649, 2002.

[18] Mattias Nordin and Per-Olof Gutman. Controlling mechanical systems with backlash–a survey. *Automatica*, 38(10):1633 – 1649, 2002.

[19] P. Rostalski, T. Besselmann, M. Baric, F. Van Belzen, and M. Morari. A hybrid approach to modelling, control and state estimation of mechanical systems with backlash. *International Journal of Control*, 80(11):1729–1740, 2007.

[20] Johannes Schiffer. Nonlinear dual motor control of a parallel kinematic robot. Master's thesis, Dept. of Automatic Control, Lund University (LTH), Sweden, 2009. ISRN LUTFD2/TFRT--5841--SE, Available at http://www.control.lth.se/publications/ .